Local Electrostatic Field Induced by the Carotenoid Bound to the Reaction Center of the Purple Photosynthetic Bacterium *Rhodobacter Sphaeroides*

Kazuhiro Yanagi, Madoka Shimizu, and Hideki Hashimoto*

"Light and Control", PRESTO/JST and Department of Physics, Graduate School of Science, Osaka City University, Osaka 558-8585, Japan

Alastair T. Gardiner, Aleksander W. Roszak, and Richard J. Cogdell

Division of Biochemistry and Molecular Biology, IBLS, University of Glasgow, Glasgow G12 8QQ, Scotland, United Kingdom

Received: July 12, 2004; In Final Form: October 25, 2004

Electroabsorption (EA) spectra were recorded in the region of the reaction center (RC) Q_y absorption bands of bacteriochlorophyll (Bchl) and bacteriopheophytin, to investigate the effect of carotenoid (Car) on the electrostatic environment of the RCs of the purple bacterium *Rhodobacter* (*Rb*.) *sphaeroides*. Two different RCs were prepared from *Rb. sphaeroides* strain R26.1 (R26.1-RC); R26.1 RC lacking Car and a reconstituted RC (R26.1-RC+ Car) prepared by incorporating a synthetic Car (3,4-dihydrospheroidene). Although there were no detectable differences between these two RCs in their near infrared (NIR) absorption spectra at 79 and 293 K, or in their EA spectra at 79 K, significant differences were detected in their EA spectra at 293 K. Three nonlinear optical parameters of each RC were determined in order to evaluate quantitatively these differences; transition dipole-moment polarizability and hyperpolarizability (*D* factor), the change in polarizability upon photoexcitation ($\Delta\alpha$), and the change in dipole-moment upon photoexcitation ($\Delta\mu^*$). The value of *D* or $\Delta\alpha$ determined for each absorption band of the two RC samples showed similar values at 77 or 293 K. However, the $\Delta\mu^*$ values of the special pair Bchls (P) and the monomer Bchls absorption bands showed significant differences between the two RCs at 293 K. X-ray crystallography of the two RCs has revealed that a single molecule of the solubilizing detergent LDAO occupies part of the carotenoid binding site in the absence of a carotenoid. The difference in the value of $\Delta\mu^*$ therefore represents the differential effect of the detergent LDAO and the carotenoid on P. The change of electrostatic field around P induced by the presence of Car was determined to be 1.7×10^5 [V/cm], corresponding to a ~10% change in the electrostatic field around P.

1. Introduction

The three-dimensional structure of the purple bacterial reaction center (RC) from *Rhodopseudomonas* (*Rps.*) *viridis* was first determined by Deisenhofer et al.[1,2] This was soon followed by the structure of the RC from *Rhodobacter* (*Rb*.) *sphaeroides*.[3,4] The RC from *Rb. sphaeroides* consists of three polypeptides called H, M, and L. All of the RC pigments are associated with the M and L subunits. This is illustrated in Figure 1. Electron transport in the RC begins when the "special pair" of bacteriochlorophyll (Bchl) molecules, P, is excited. The electron moves from P down the A branch. The pseudo 2-fold symmetrically arranged B branch does not participate in electron transport. Why the electron only goes down the A branch has been a major topic or research since the structure of the RC was first described.

Car is located ~16 Å from P on the B branch side and is bound in a twisted 15−15′-cis configuration.[5] Since the distance between the 15−15′-cis double bond of Car and the accessory Bchl on the B branch (B_B) is 3.2−3.4 Å, Car is in van der Waals contact with B_B.[5] Singlet excitation energy is transferred from Car to P through B_B,[6] whereas triplet excitation energy is transferred from P to Car through B_B.[7] The former process is defined as the light-harvesting function of Car (observed also in light-harvesting complexes) since Car absorbs light in the spectral region, 400−600 nm, where Bchls have low extinction coefficients. The latter process reflects the photoprotective function of Car, as this transfer process prevents the generation

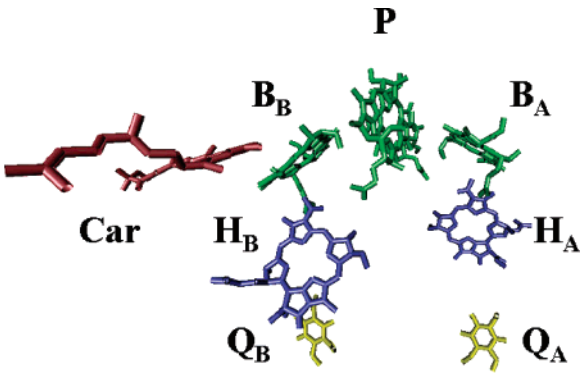

Figure 1. Spatial arrangement of the pigments in the *Rb. sphaeroides* RC; P, bacteriochlorophyll (Bchl) dimer; B_A, B_B, Bchl monomers; H_A, H_B, bacteriopheophytins; Q_A, Q_B, ubiquinones; Car, Carotenoid. This figure was drawn by using VMD program[53] based on PDB (protein data bank) data; 1K6L.

* To whom correspondence should be addressed. Phone & Fax: +81-6-6605-2526. E-mail: hassy@sci.osaka-cu.ac.jp.

10.1021/jp046929d CCC: $30.25
Published on Web 12/24/2004

of destructive singlet oxygen.[8] Although the mechanisms of these two functions of the Car have been well investigated,[8,9] the role of Car on unidirectional electron transfer has received scant attention. It appears that Car does not directly impinge on electron transfer, rather unidirectional electron transfer occurs regardless of the presence of Car.[10] Therefore, we asked the question whether the asymmetry induced by the presence of the Car could contribute to the asymmetry in the electrostatic environment around the pigments between the A and B branches and as a consequence indirectly affect the electron-transfer process.

Nonlinear optical properties of materials are sensitive to the change of local electrostatic environment.[11] Electroabsorption (EA) spectroscopy is one of the most suitable methods to determine the nonlinear optical parameters. The following three nonlinear optical parameters can be determined from EA spectroscopy;[12,13] transition dipole-moment polarizability and its hyperpolarizability (*D* factor), the change of polarizability upon photoexcitation ($\Delta\alpha$), and the change of dipole-moment upon photoexcitation ($\Delta\mu$). Electroabsorption spectroscopy has been applied to RC from the early 1980s.[11,14−29] (for excellent reviews interested readers should consult Boxer et al.[30,31]). The most remarkable characteristic of the nonlinear optical property of RC is the large $\Delta\mu$ value of P, initially assumed to be caused by mixing with the charge transfer (CT) state.[21−23] However, Middendorf et al.[11] pointed out that a strong local electric field can also induce such enhancement of $\Delta\mu$ and estimated that the local electric field around P to be more than 1.2×10^6 [V/cm].[11] They proposed that the amplitude of the local electric field would be evaluated from the nonlinear optical parameters determined from EA spectroscopy. Therefore, any change of the electric field due to the presence of Car around P could in principle be detected by comparing the nonlinear optical parameters of RC containing (R26.1-RC + Car) and lacking Car (R26.1-RC). To test this hypothesis, the EA spectra of these two RC samples were investigated. We have based our study on the RC with the synthetic carotenoid (3,4-dihydrospheroidene) rather than the RC with the native carotenoid (spheroidene), as we have recently determined the crystal structure of the RC in which 3,4-dihydrospheroidene has been incorporated[5] and we had plenty of this sample available in our laboratory. This is also a good choice because R26.1 is an ill-defined mutant. It is certainly not a point mutation, so in some ways R26.1 with or without Car is a better control than R26.1 vs wild-type RC, for example, from *Rb. sphaeroides* 2.4.1.

2. Materials and Methods

2.1. Preparation of the RC from *Rb. sphaeroides* R-26.1. Whole cells of *Rb. sphaeroides* R-26.1 were grown anaerobically in modified Huntner's media,[32] harvested by low speed centrifugation, and resuspended in 20 mM Tris HCl, pH 8.0. After the addition of a very small quantity of DNase (Sigma) and $MgCl_2$, the cells were thoroughly homogenized before being disrupted by passage (2×) through a French Pressure cell at 14 000 psi. Any cells wall debris was pelleted by a 10 min low-speed spin and discarded. Chromatophore membranes were then pelleted by a high-speed centrifugation spin (2 000 000 g, 90 min) and the supernatant discarded. The chromatophores were re-suspended with 20 mM Tris HCl, pH 8.0 and adjusted to an NIR $OD_{874} = 50$. The detergent lauryldimethylamine oxide (LDAO) was added dropwise to give a concentration of 0.3% (v/v) and the solution stirred gently in the dark for 1 h at 26 °C, after which any unsolubilized material was removed by centrifugation. The solubilized RC complex was then loaded onto an ion-exchange (DE52, Whatman) column and eluted by increasing the concentration of NaCl. The final, purified RC complex had a purity ratio (OD_{280}/OD_{800}) of less than 2.0.

2.2. Incorporation of Carotenoids into the RC from *Rb. sphaeroides* R-26.1. The 3,4-dihydrospheroidene was synthesized as previously described.[33−35] The RCs (NIR $OD_{800} = 14.5$) were adjusted to a final concentration of 0.67% (v/v) LDAO, 20 mM Tris HCl, pH 8.0. A 15-fold molar excess of 3,4-dihydrospheroidene in petroleum ether relative to BChl was layered onto the surface of the RC solution. The petroleum ether was then evaporated under a stream of nitrogen. The resulting mixture was sonicated for 45 min at room temperature in the dark. The solution was then diluted five-times with 15 mM Tris HCl, pH 8.0, and loaded onto a DE52 ion-exchange column. The RCs containing the bound carotenoid were washed with 0.05% (v/v) LDAO, 20 mM Tris HCl, pH 8.0 to remove the excess unbound carotenoid. The RCs containing incorporated Car were then eluted with buffer containing 300 mM NaCl, 0.05% (v/v) LDAO, 20 mM Tris HCl, pH 8.0 and dialyzed overnight in Spectrapor standard cellulose dialysis tubing (25 mm, MW cutoff 12 000−14 000 D) against 0.05% (v/v) LDAO, 20 mM Tris HCl, pH 8.0. X-ray crystallography was used to investigate the location of the reconstituted Car molecule and to test whether it was bound to the RC in a manner similar to the carotenoid in wild-type carotenoid containing RCs (Protein Data Bank ID: 1RQK).[5] According to the results of X-ray crystallography, both R26.1-RC and R26.1-RC + Car contain equivalent ubiquinone occupancy in the Q_A and Q_B binding sites. It was assumed that the redox state of R26.1-RC + Car is equivalent to R26.1-RC since they had a similar relative absorbance at 870 nm. The degree of reconstitution of the carotenoid was estimated to be ~90% based on a comparison of the ratio of the carotenoid absorbance in R26.1-RC + Car with that in the neurosporene containing RC from *Rb. sphaeroides* G1C, neurosporene having the same conjugated backbone as 3,4-dihydrospheroidene.

2.3. Optical Spectroscopy. RC complexes were dispersed isotropically in poly(vinyl alcohol) (PVA) films (PVA-217, Kuraray Co., Ltd), and electroabsorption (EA) and standard absorption spectra were recorded. These films were prepared as follows. Both the RC complexes ($OD_{800} = 5$) and the PVA polymer (1%) were dissolved in 20 mM Tris HCl, 0.05% (v/v) LDAO, pH 8.0. A small aliquot of this solution was then dropped onto the surface of a glass substrate, on which gold electrodes (gap distance is 50−100 μm, thickness of the electrodes is ~0.2 μm) had been installed. The gap distance between the electrodes was determined by optical microscopy to an accuracy of 2 μm. Any residual solvent was then removed under reduced pressure. The optical absorption spectra were recorded using a UV/vis spectrophotometer (JASCO, V-530). EA spectra were recorded in the setup described previously.[25,36,37] Absorbance changes (ΔA) induced by the applied electric field were then calculated by using the following equation, $\Delta A = -\ln[(I + \Delta I)/I]/2.303$. Here I is the intensity of transmitted light. The temperature dependence of the EA spectra was studied using a temperature-controlled liquid-nitrogen cryostat (Oxford, Optistat-DN). The sample temperature was set to 79 or 293 K with an accuracy of ±0.1 K.

2.4. Theoretical Model to Analyze the EA Spectra. Although the general theory of EA spectroscopy is relatively well developed,[12,13] a fuller theoretical understanding of it within the biological context is required. This is needed in order to facilitate correlation of the measured spectra with the structure of the pigment−protein interactions and how these affect the

magnitude of the experimentally determined nonlinear optical parameters (D factor, $\Delta\alpha$, and $\Delta\mu$). This study investigated the change in the electrostatic field around the RC pigments induced by the presence of Car and its affect on the optical nonlinearity of these pigments. To investigate these effects, a theoretical model has been developed based on the background theory originally described by Liptay.[12,13]

The ground and excited states of a pigment are denoted as $|0\rangle$ and $|1\rangle$ respectively. The electric field, $\mathbf{F}$, affecting the electronic state of P is considered as a linear combination of the following three components; the applied electric field ($\mathbf{F}_a$), the pocket field due to the presence of apoproteins ($\mathbf{F}_p$) and the electrostatic field induced by the presence of Car ($\mathbf{F}_c$)[38]

$$\mathbf{F} = \mathbf{F}_a + \mathbf{F}_p + \mathbf{F}_c \tag{1}$$

Here $\mathbf{F}$, $\mathbf{F}_a$, $\mathbf{F}_p$, and $\mathbf{F}_c$ indicate vectors.

Although the idea to describe the electrostatic field as a summation of the applied and pocket fields has been already suggested,[38] the $\mathbf{F}_c$ term has been introduced additionally in order to clarify the effect of the presence of Car on the electrostatic environment of the pigments.

According to eq 1, the shift of the $|0\rangle \rightarrow |1\rangle$ transition energy induced by the electrostatic field (Stark shift), $\Delta\nu_{01}$, is written as[38]

$$\begin{aligned} h\Delta\nu_{01} &= -\Delta\boldsymbol{\mu}\mathbf{F} - \frac{1}{2}\Delta\alpha\mathbf{F}^2 \\ &= -\Delta\boldsymbol{\mu}^*\mathbf{F}_a - \frac{1}{2}\Delta\alpha\mathbf{F}_a{}^2 - (\Delta\boldsymbol{\mu} + \Delta\alpha\mathbf{F}_p)\mathbf{F}_c - \\ &\qquad \frac{1}{2}\Delta\alpha\mathbf{F}_c{}^2 - \Delta\boldsymbol{\mu}\mathbf{F}_p - \frac{1}{2}\Delta\alpha\mathbf{F}_p{}^2 \end{aligned} \tag{2}$$

$$\Delta\boldsymbol{\mu}^* = \Delta\boldsymbol{\mu} + \Delta\alpha(\mathbf{F}_p + \mathbf{F}_c) \tag{3}$$

It should be noted that the $\mathbf{F}_c$ term directly affects the transition frequency. According to eq 2, the shift of the transition energy due to $\mathbf{F}_c$, $h\Delta_c\nu_{01}$, can be written as

$$h\Delta_c\nu_{01} \approx -(\Delta\boldsymbol{\mu} + \mathbf{F}_p\Delta\alpha)\mathbf{F}_c \tag{4}$$

This shift can be detected by comparing the difference in the absorption spectra of R26.1-RC and R26.1-RC + Car.

Then the transition dipole-moment between the ground and excited states in the presence of the electrostatic field, $\tilde{\boldsymbol{\mu}}_{01}$, can be approximately written as

$$\tilde{\boldsymbol{\mu}}_{01} = \boldsymbol{\mu}_{01} + \mathbf{X}\mathbf{F} + \frac{1}{2}\mathbf{Y}\mathbf{F}^2 \approx \boldsymbol{\mu}_{01} + \mathbf{X}\mathbf{F}_a + \frac{1}{2}\mathbf{Y}\mathbf{F}_a{}^2 \tag{5}$$

Here $\boldsymbol{\mu}_{01}$ is the transition dipole-moment in the absence of an electrostatic field. $\mathbf{X}$ and $\mathbf{Y}$ are the transition dipole-moment polarizability and hyper-polarizability respectively in the absence of the electrostatic field.

In this study, the RC was dispersed and fixed in a PVA polymer matrix and then the magic angle technique was applied. After averaging over the whole ensemble of sample orientations, the absorption change due to the applied electric field $\mathbf{F}_a$, ΔA, can be written as[39]

$$\Delta A = \left(\frac{1}{3}DA + \frac{1}{6}F\frac{dA/\nu}{d\nu} + \frac{1}{6}|\Delta\boldsymbol{\mu}^*|^2\frac{d^2A/\nu}{d\nu^2}\right)|\mathbf{F}_a|^2 \tag{6}$$

and

$$D = \frac{1}{|\boldsymbol{\mu}_{01}|^2}(\mathbf{X}^2 + \boldsymbol{\mu}_{01}\mathbf{Y}) \tag{7}$$

$$F = Tr[\Delta\alpha] + 2\frac{\boldsymbol{\mu}_{01}\mathbf{X}}{|\boldsymbol{\mu}_{01}|^2}\Delta\boldsymbol{\mu}^* \approx Tr[\Delta\alpha] \tag{8}$$

Equation 6 indicates that ΔA can be written as a linear combination of the zero-, first-, and second-order derivatives of A. This equation corresponds to the theoretical formulation of ΔA developed by Liptay,[12] except that $\Delta\boldsymbol{\mu}$ is replaced with $\Delta\boldsymbol{\mu}^*$. In eq 8, it is assumed that $\Delta\alpha$ will be the dominant contribution to the F value since the contribution of the D factor to the optical nonlinearity is expected to be small ($\mathbf{X} \sim 0$).[11]

There are two important implications arising from eq 6: the coefficients of the zero- and first-order derivative components (the D and Tr[$\Delta\alpha$] values) are not affected by $\mathbf{F}_c$ and the coefficient of the second-order derivative ($\Delta\boldsymbol{\mu}^*$) depends on the $\mathbf{F}_c$ value.

According to eq 3, the change of the $\Delta\boldsymbol{\mu}^*$ value due to the presence of $\mathbf{F}_c$ ($\Delta_c\boldsymbol{\mu}^*$) can be written as

$$\Delta_c\boldsymbol{\mu}^* = \Delta\alpha\mathbf{F}_c \tag{9}$$

Therefore, the $\Delta_c\boldsymbol{\mu}^*$ value can be determined from the difference of $\Delta\boldsymbol{\mu}^*$ values between the carotenoidless and the carotenoid-containing RCs. Since the $\Delta\alpha$ value can be also estimated from the EA spectra, the magnitude of $\mathbf{F}_c$ can be quantitatively evaluated by using eq 9.

2.5. Analysis of the EA Spectra. To determine the values of D, Tr[$\Delta\mathbf{a}$], and $\Delta\mathbf{m}^*$, a multiregression analysis was used to simulate the wave forms of the EA spectra using a linear combination of the zero-, first-, and second-order derivatives of the absorption spectra (hereafter called waveform analysis). According to eq 6, the coefficients of these derivative components correspond to the D, Tr[$\Delta\alpha$], and $\Delta\mu^*$ values. However, it is important to recognize that eq 6 assumes, implicitly, uniform nonlinearity over the entire absorption band.[25,37,40−42] If this assumption is not valid, as sometimes happens when an absorption band is composed of several subbands, a deconvolution protocol is required to determine the nonlinear optical parameters of each individual subband.[37] As discussed in the subsequent section, the higher-order vibronic, as well as upper excitonic, transitions of the P band overlap in the spectral region of the B and H bands, and so it is not simple to evaluate the nonlinear optical properties of the B and H bands from their EA spectra. Therefore, to overcome this problem, the present study concentrated solely on the nonlinear optical properties of the P band.

2.6. Dual-Phase Lock in Detection. Most previous reports on the use of Stark spectroscopy to study photosynthetic pigment−protein complexes have reported only in-phase signals.[11,14−23,26−28,43−46] Although these studies have been very informative, more detailed information on the dynamic electrostatic interactions with the environment can be obtained from the out-of-phase (quadrature-phase) signals. Stark spectra of J-aggregates of a pseudo-isocyanine dye (1,1′-diethyl-2,−2,2′-quinocyanine bromide) showed the first clear evidence of the presence of a quadrature-phase signal.[47,48] We also reported the presence of the quadrature-phase EA signals in LH2 complex from *Rb. sphaeroides* strain G1C using dual-phase lock-in detection.[25] Indeed, this study suggested that the pigment−protein interaction was one of the factors that generates the phase-retarded signals.[25] Based on this result, the presence of

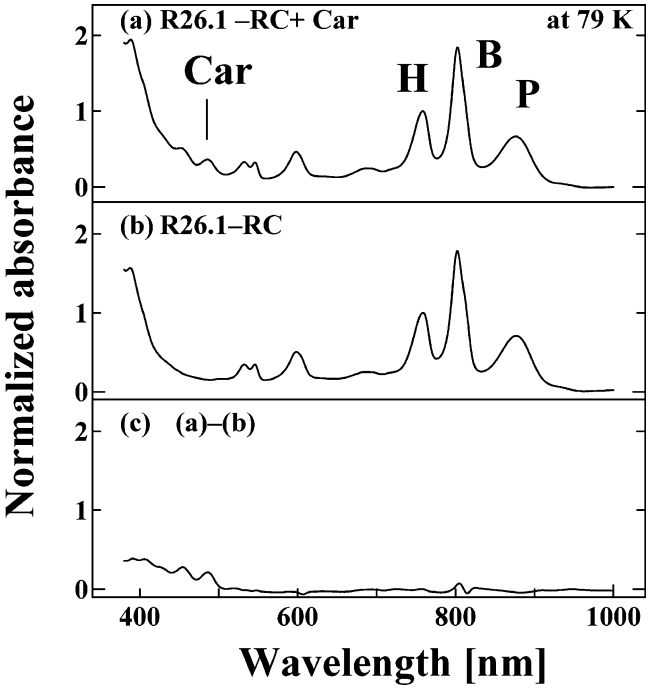

Figure 2. Absorption spectra of (a) R26.1-RC and (b) R26.1-RC + Car at 79 K RCs dispersed into PVA matrix. These spectra are normalized at the maxima of H band (at 760 nm). The differential absorption spectrum between the two spectra is shown in part c.

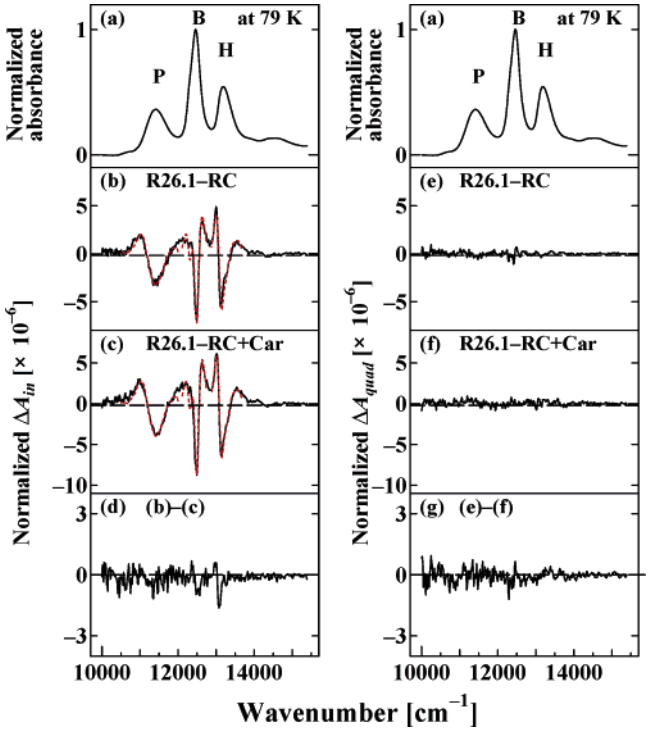

Figure 3. In- and quadrature-phase EA spectra of R26.1-RC and R26.1-RC + Car at 79 K. (a) Absorption spectra of R26.1-RC, (b) and (c) in-phase EA spectra (solid lines) of R26.1-RC and R26.1-RC + Car and the results of waveform analyses (dotted red lines). After the normalization procedure (see section 3.2.1), the differential EA spectrum, (d), between panels b and c was derived. Panels e and f show the quadrature-phase EA spectra (solid lines) of R26.1-RC and R26.1-RC+Car and the results of waveform analyses (dotted lines). After the normalization procedure, the differential EA spectrum, (g), between (e) and (f) was derived.

similar phase-retarded signals of the EA spectra of RCs have been investigated using dual-phase lock-in detection.

3. Results and Discussion

3.1. Absorption Spectra. Figure 2, parts a and b, shows absorption spectra of R26.1-RC and R26.1-RC + Car at 79 K. The observed absorption bands near 880, 800, and 760 nm are due to the Q_y transitions of P, B, and H, respectively.[49] Hereafter these three absorption bands are denoted as P, B, and H, respectively. To compare these two spectra, they were normalized at the maxima of the H band (at 760 nm), and then the difference spectrum was derived as shown in Figure 2c. The absorption band of Car can be clearly identified in this difference spectrum. However, since the difference between the two spectra is so small in the region of the P, B, and H bands, it is not possible to measure any shift of their transition energies due to $\mathbf{F}_c$.

3.2. EA Spectroscopy. *3.2.1. EA Spectra at 79 K.* Figure 3, parts b and c, shows the in-phase EA spectra of the R26.1-RC and R26.1-RC + Car at 79 K. The solid lines are the experimental observations and the dotted red lines are the result of the waveform analyses. Since the P, B, and H bands were well resolved at 79 K (as shown in Figure 3a) the EA spectra of the three bands were analyzed using their observed absorption line shapes. The nonlinear parameters obtained are listed in Table 1.

As is shown in eq 6, the amplitude of ΔA depends linearly on $|\mathbf{F}_a|^2$ and A. Therefore, to compare the two EA spectra, they were normalized to the same values of $|\mathbf{F}_a|^2$ and A. Figure 3d shows the normalized difference EA spectrum. Since the difference between the EA spectra of two RCs is barely detectable at 79 K, it is not possible to determine the effect of $\mathbf{F}_c$ on the pigments from these results.

Since modulation of the position of polar amino acid residues in response to the applied electric field was suggested as a possible mechanism for the generation of phase-retarded signals, it might be expected that this effect would be strongly temperature dependent.[25] Accordingly, the quadrature-phase signals were not observed at 79 K with the LH2 complex from *Rb. sphaeroides* G1C.[25] Therefore, it was not unexpected that quadrature-phase signals could not be detected at 79 K with RCs. Figure 3e−g shows quadrature-phase EA spectra of R26.1-RC and R-26-RC + Car and their difference spectrum. As predicted, no quadrature-phase signals were observed in either case.

3.2.2. EA Spectra at 293 K. Figure 4a shows the experimentally observed absorption spectrum of R26.1-RC (solid line) at 293 K. The P, B, and H bands (dotted lines) were deconvoluted from the full spectrum using Gaussian functions. Parts b and c of Figure 4 are the in-phase EA spectra of R26.1-RC and R26.1-RC + Car at 293 K. The solid lines are the experimentally observed spectra, and the dotted red lines are the result of waveform analyses. Since the P, B, and H bands are expected to have different optical nonlinearity,[23] the EA spectra were reproduced by using linear combinations of the zero-, first-, and second-order derivatives of each separate absorption band. The nonlinear optical parameters determined by these analyses are listed in Table 1. The difference spectrum between parts b and c of Figure 4, produced by the same normalization procedure described in 3.2.1, is shown in Figure 4d. In contrast to the case at 79 K, a significant difference between the EA spectra of the two RCs could be observed. This difference spectrum, in the region of the P band, resembles the second-order derivative form and indicates that the $\Delta\boldsymbol{\mu}^*$ values are different between the two RCs.

TABLE 1: Nonlinear Optical Parameters Determined from the Waveform Analyses of EA Spectra

	P band	D [10^{-18} [(m/f_LV)^2]]	Tr[$\Delta\alpha$] [Å^3/f_L^2]	$\Delta\mu^*$ [D/f_L]
79 K	R26.1-RC	-1.5 ± 0.4	$(2.2 \pm 0.3) \times 10^2$	6.5 ± 0.3
	R26.1-RC + Car	-1.8 ± 0.4	$(2.4 \pm 0.8) \times 10^2$	6.5 ± 0.5
293 K	R26.1-RC	3.9 ± 0.4	$-(1.7 \pm 0.1) \times 10^3$	10.8 ± 0.4
	R26.1-RC + Car	3.6 ± 0.5	$-(1.7 \pm 0.4) \times 10^3$	9.0 ± 0.4
	B band	D [10^{-18} [(m/f_LV)^2]]	Tr[$\Delta\alpha$] [Å^3/f_L^2]	$\Delta\mu^*$ [D/f_L]
79 K	R26.1-RC	0.9 ± 0.2	$-(1.2 \pm 0.4) \times 10^2$	2.8 ± 0.3
	R26.1-RC + Car	1.4 ± 0.5	$-(1.1 \pm 0.2) \times 10^2$	2.9 ± 0.2
293 K	R26.1-RC	-7.1 ± 0.5	$-(5.3 \pm 3.6) \times 10$	2.1 ± 0.1
	R26.1-RC + Car	-7.0 ± 1.7	$-(5.8 \pm 2.4) \times 10$	1.5 ± 0.2
	H band	D [10^{-18} [(m/f_LV)^2]]	Tr[$\Delta\alpha$] [Å^3/f_L^2]	$\Delta\mu^*$ [D/f_L]
79 K	R26.1-RC	0.4 ± 0.2	$-(8.4 \pm 7.2) \times 10$	4.4 ± 0.3
	R26.1-RC + Car	0.4 ± 0.1	$-(0.9 \pm 2.0) \times 10$	4.3 ± 0.3
293 K	R26.1-RC	0.8 ± 0.2	$(9.5 \pm 2.3) \times 10$	6.2 ± 0.4
	R26.1-RC + Car	0.8 ± 0.3	$(10.0 \pm 4.0) \times 10$	5.7 ± 0.5

Figure 4, parts e and f, shows the quadrature-phase EA spectra of R26.1-RC and R26.1-RC + Car at 293 K. Again in contrast to the case at 79 K, quadrature-phase signals were observed at 293 K. At this temperature, the presence of the phase-retarded signal indicates the presence of an electrostatic interaction between pigments and their surrounding protein environment.[25] Figure 4g shows the difference EA spectrum between parts e and f. A small difference between the two RCs was observed and reflects the fact that the Car induced a change in the electrostatic environment of P. However, a full discussion of the physical implications of these phase-retarded signals is beyond the scope of the present study and will be presented elsewhere.

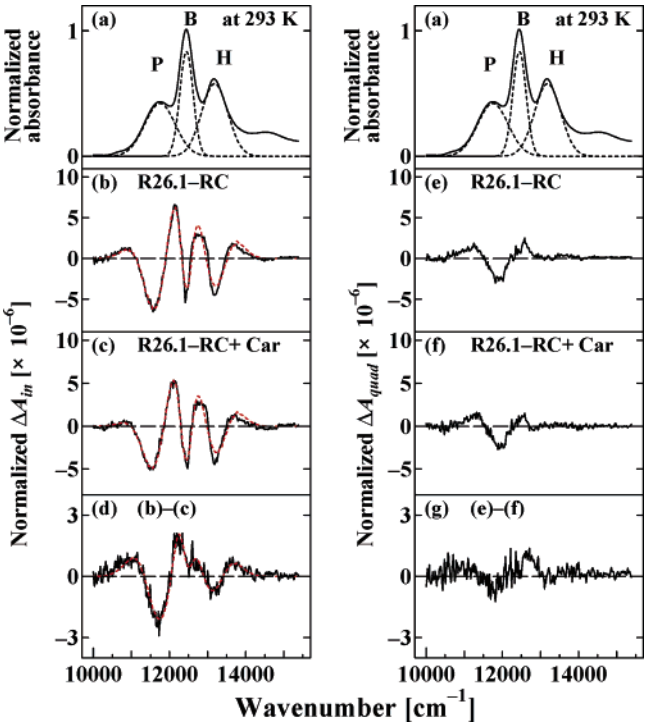

Figure 4. In- and quadrature-phase EA spectra of R26.1-RC and R26.1-RC + Car at 293 K. Panel a shows absorption spectrum (solid line) of R26.1-RC and the P, B, and H bands determined from the deconvolution by using Gaussian functions (dotted lines). Panels b and c show the in-phase EA spectra (solid lines) of R26.1-RC and R26.1-RC+Car and the results of waveform analyses (dotted red lines). After the normalization procedure (see section 3.2.1), the differential EA spectra, (d), between panels b and c was derived. Panels e and f show the in-phase EA spectra (solid lines) of R26.1-RC and R26.1-RC+Car and the results of waveform analyses (dotted red lines). After the normalization procedure, the differential EA, (g), spectra between panels e and f was derived.

3.2.3. Nonlinear Optical Parameters of the P, B, and H Bands. The nonlinear optical parameters of the P, B, and H bands determined from the EA spectra are listed in Table 1. As is mentioned in section 2.5, we have focused our attention on the nonlinear optical parameters of the P band. The reported $\Delta\mu$ value of the P band at room temperature (RT) is 8.9−11.2 [D/f_L].[21−23] This reduces to 5.0−7.5 [D/f_L][11,21−23] at 77 K. Here f_L is a local electric field correction factor. Values of Tr[$\Delta\alpha$] and D at 77 K have been reported; Tr[$\Delta\alpha$] = 750 − 1230 [Å^3/f_L^2][11,14] and $D = -4.53 \cdot 10^{-18}$ [3(−1.51 × 10^{-18})] [(m/f_LV)^2].[14] However, as far as we know, the Tr[$\Delta\alpha$] and D values at RT have not been reported. It is known that differences in sample preparation and analysis methods affect the values of these nonlinear optical parameters.[15,19] For example, the values depend on the solvent in which the RCs are dissolved[15,19] and sometimes would be overestimated if the zero and first derivative contributions are neglected.[11] When such factors are taken into account, the derived values listed in Table 1 are consistent with the reported values.

In eq 5, the contribution of $\mathbf{F}_c$ and $\mathbf{F}_p$ was ignored in order to simplify the model. If this simplification is not valid, according to the discussion in section 2.4, the differences between R26.1-RC and R26.1-RC + Car will be observed in the values of the D and F terms. However, when the experimental errors are taken into consideration, both the D and F (the value of F corresponds to Tr[$\Delta\mathbf{a}$] value listed in Table 1) terms for the two RCs are found to be similar. Therefore, the above simplification has proved to be valid.

The most remarkable features present in Table 1 are the values of $\Delta\boldsymbol{\mu}^*$ of the P and B bands at 293 K. Even allowing for experimental error, there are significant differences in these values between the two RCs. According to eq 9, this result clearly indicates the effect of $\mathbf{F}_c$ on the $\Delta\boldsymbol{\mu}^*$ values of the P and B bands.

As is mentioned in section 2.5, only the nonlinear optical properties of the P band are discussed in detail. There is about 1.0 [D/f_L] difference between the two RCs in the $\Delta\boldsymbol{\mu}^*$ values at 293 K and, according to eq 9, this difference corresponds to $\boldsymbol{\Delta}_c\boldsymbol{\mu}$. Based on eq 9, using the Tr[$\Delta\alpha$] value of -2.1×10^3 [Å^3/f_L^2] at 293 K, the $\mathbf{F}_c$ value was estimated to be 1.7×10^5 [V/cm]. In this calculation, the experimental error is taken into

account for the minimum order estimation of $\mathbf{F}_c$, and the reported f_L value of 1.2 was used.[21,22] The magnitude of the local field around P has been reported to be more than 1.2×10^6 [V/cm].[11] Thus, the present result indicates that the presence of Car induces up to a 10% change of the electrostatic environment around P. Due to the uncertainty in the reported value of the local field around P, this estimate probably represents an upper limit of the effect of the Car.[12] This uncertainty also means that it is not possible to determine error bars for this upper limit.

X-ray crystallography of carotenoidless R26.1-RC and R26.1-RC + Car has shown that structurally the difference between these RCs is not simply the presence or absence of Car:[5] conformational changes of the phytol tail and of individual amino acid residues also occur. In the carotenoidless R26.1-RC, the central portion of the Car binding pocket was found to contain a stretch of electron density that was fitted with a single LDAO molecule. The difference in the strength of the electrostatic field experienced by P and B_B in R26.1-RC and R26.1-RC + Car is due to the presence or absence of Car. However, it is not yet possible to distinguish between a direct interaction between Car and P and B_B and an effect mediated by the change in the conformations of the amino acid residues and the phytol chain that occur in the presence of Car.

The ground-state dipole-moments of LDAO and 15-cis Car are semiempirically calculated to be 5.2 and 2.2 [D], respectively, by using MOPAC 2000 ver. 1.11 with an AM1 Hamiltonian. The Car binding site is located ~20 Å away from P. Despite this distance, it is known that the oxidized special pair, P^+, can cause a shift in the absorbance bands of the RC Car.[50,51] It is reasonable, therefore, to suggest that the electric field induced by the ground-state dipole-moment of a molecule present in the Car binding pocket can also affect P. If the influence of the Car represents such a direct interaction with P, then, since in the absence of the Car part of the binding site is occupied by LDAO, the difference of the dipole-moments between LDAO and Car must be responsible for the difference of the electrostatic field sensed by P. This difference in the electrostatic field can be estimated to be $\sim 1.1 \times 10^5$ [V/cm] by using equations that describe the electric field generated by dipole-moments.[52] Here a value of unity was assumed for the relative dielectric constant. This value is quite consistent with the experimentally determined $\mathbf{F}_c$ value, 1.7×10^5 [V/cm]. The dipole moment of the LDAO is larger than that of Car. Hence, it is expected that the effect of Car is to decrease the electrostatic field around P. However, it is difficult to decide whether the Car decreases or increases the asymmetry of the field around P, which is the key issue. Since the effect of the presence or absence of Car on the charge separation process has not been studied in detail, further investigations are required to investigate this interesting issue.

Finally, the effect of $\mathbf{F}_c$ on the absorption and EA spectrum at 79 K has been evaluated using the determined $\mathbf{F}_c$ value, 1.7×10^5 [V/cm].

(1) According to eq 4, the shift of the transition energy due to $\mathbf{F}_c$, $\Delta_c\nu_{12}$, can be estimated to be 22 cm^{-1} at 293 K and 15 cm^{-1} at 79 K, using the $\Delta\boldsymbol{\mu}^*$ values 9.0 [D/f_L] at 293 K and 6.5 [D/f_L] at 79 K. These shifts correspond to about 0.1 at 293 K and 0.25 at 79 K of the respective thermal fluctuation energies (~200 cm^{-1} at 293 K and ~60 cm^{-1} at 79 K). Since the resolution of our absorption spectra is ~20 [cm^{-1}] in the spectral region of the P and B bands, the identification of $\Delta_c\nu_{12}$ is not possible in the present experiments, and so differences in the absorption spectra at 79 K between R26.1-RC and R26.1-RC+Car were not observed.

(2) The change of $\Delta\boldsymbol{\mu}^*$ due to $\mathbf{F}_c$, $\Delta_c\boldsymbol{\mu}^*$ at 79 K can be estimated to be ~0.1 [D/f_L] by using the experimentally determined Tr[$\Delta\mathbf{a}$] value, 2.4×10^2 [$Å^3/f_L^2$]. This change is smaller than the experimental error (±0.3 [D/f_L]); thus, $\Delta_c\boldsymbol{\mu}^*$ could not be detected. This is the reason no difference could be detected in the EA spectra at 79 K between the two RCs, in contrast to the situation at 293 K.

4. Conclusion

Although no differences were observed between the absorption and EA spectra of R26.1-RC and R26.1-RC+Car at 79 K, significant differences were detected between their EA spectra at 293 K. At 293 K, the absorption spectra of the two RCs in the NIR remained the same. Spectral analyses showed that both the *D* and Tr[$\Delta\alpha$] values were found to have similar values for the two RCs. However, it was possible to detect a difference in the $\Delta\boldsymbol{\mu}^*$ values of the P and B bands in two RCs. This clearly indicates that the presence of Car effects the electrostatic environment around P and B_B. Based on our theoretical model, the electrostatic field on P induced by Car corresponds to about a 10% change of the total electrostatic field around P. Since Car disturbs the pseudo 2-fold symmetry of RC, the resulting electrostatic effect induced by Car on P is also likely to be asymmetric. However, since the unidirectionality of the primary electron transfer reactions in the RCs takes place successfully irrespective of the presence or absence of the RC Car. The extra electrostatic field induced by this Car may enhance the asymmetric character of this electrostatic field although it cannot be a major determinant of this unidirectionality. It is expected that similar electrostatic effects induced by Car on P will also be observed in RCs containing native carotenoids. Further experiments on the effect of Car are currently in progress.

Acknowledgment. H.H. thanks Grant-in-aid from the Japanese Ministry of Education, Culture, Sports, Science & Technology (Grant Nos. 14340090 and 14654072). H.H. and R.J.C. thank the Grant-in-aid from BBSRC and NEDO international joint-research. This work is supported in part by the grant from Nakatani Electronic Measuring Technology Association of Japan.

References and Notes

(1) Deisenhofer, J.; Epp, O.; Miki, K.; Huber, R.; Michel, H. *J. Mol. Biol.* **1984**, *180*, 385.
(2) Deisenhofer, J.; Epp, O.; Miki, K.; Huber, R.; Michel, H. *Nature* **1985**, *318*, 618.
(3) Allen, J. P.; Feher, G.; Yeates, T. O.; Komiya, H.; Rees, D. C. *Proc. Natl. Acad. Sci. U.S.A.* **1987**, *84*, 5730.
(4) Allen, J. P.; Feher, G.; Yeates, T. O.; Komiya, H.; Rees, D. C. *Proc. Natl. Acad. Sci. U.S.A.* **1987**, *84*, 6162.
(5) Roszak, A. W.; McKendrick, K.; Gardiner, A. T.; Mitchell, I. A.; Isaacs, N. W.; Cogdell, R. J.; Hashimoto, H.; Frank, H. A. *Structure* **2004**, *12*, 765.
(6) Lin, S.; Katilius, E.; Taguchi, A. K. W.; Woodbury, N. W. *J. Phys. Chem. B* **2003**, *107*, 14103.
(7) Cogdell, R. J.; Monger, T. G.; Parson, W. W. *Biochim. Biophys. Acta* **1975**, *408*, 189.
(8) Angerhofer, A.; Bornhauser, F.; Aust, V.; Hartwich, G.; Scheer, H. *Biochim. Biophys. Acta* **1998**, *1365*, 404.
(9) Fraser, N. J.; Hashimoto, H.; Cogdell, R. J. *Photosynth. Res.* **2001**, *70*, 249.
(10) Yeates, T. O.; Komiya, H.; Rees, D. C.; Allen, J. P.; Feher, G. *Proc. Natl. Acad. Sci. U.S.A.* **1987**, *84*, 6438.
(11) Middendorf, T. R.; Mazzola, L. T.; Lao, K.; Steffen, M. A.; Boxer, S. G. *Biochim. Biophys. Acta* **1993**, *1143*, 223.
(12) *Excited States*; Liptay, W., Ed.; Academic Press: New York, 1974; p 129.

(13) Liptay, W.; Wortmann, R.; Schaffrin, H.; Burkhard, O.; Reitinger, W.; Detzer, N. *Chem. Phys.* **1988**, *120*, 429.
(14) Beekman, L. M. P.; Steffen, M. A.; van Stokkum, I. H. M.; Olsen, J. D.; Hunter, C. N.; Boxer, S. G.; van Grondelle, R. *J. Phys. Chem. B* **1997**, *101*, 7284.
(15) Beekman, L. M. P.; Frese, R. N.; Fowler, G. J. S.; Picorel, R.; Cogdell, R. J.; van Stokkum, I. H. M.; Hunter, C. N.; van Grondelle, R. *J. Phys. Chem. B* **1997**, *101*, 7293.
(16) Braun, H. P.; Michel-Beyerle; Breton, J.; Buchanan, S.; Michel, H. *FEBS. Lett* **1987**, *221*, 221.
(17) De Leeuv, D.; Mally, M.; Buttermann, G.; Okamura, M. Y.; Feher, G. *Biophys. J.* **1982**, *37*.
(18) DiMagno, T. J.; Bylina, E. J.; Angerhofer, A.; Youvan, D. C.; Norris, J. R. *Biochemisty* **1990**, *29*, 899.
(19) Gottfried, D. S.; Steffen, M. A.; Boxer, S. G. *Biochim. Biophys. Acta* **1991**, *1059*, 76.
(20) Hammes, S. L.; Mazzola, L. T.; Boxer, S. G.; Gaul, D. F.; Schenck, C. C. *Proc. Natl. Acad. Sci. U.S.A.* **1990**, *87*, 5682.
(21) Lockhart, D. J.; Boxer, S. G. *Biochemisty* **1987**, *26*, 664.
(22) Lockhart, D. J.; Boxer, S. G. *Proc. Natl. Acad. Sci. U.S.A.* **1988**, *85*, 107.
(23) Lösche, M.; Feher, G.; Okamura, M. Y. *Proc. Natl. Acad. Sci. U.S.A.* **1987**, *84*, 7537.
(24) Steffen, M. A.; Lao, K.; Boxer, S. G. *Science* **1994**, *264*, 810.
(25) Yanagi, K.; Hashimoto, H.; Gardiner, A. T.; Cogdell, R. J. *J. Phys. Chem. B* **2004**, 108, 10334.
(26) Zhou, H.; Boxer, S. G. *J. Phys. Chem. B* **1998**, *102*, 9139.
(27) Zhou, H.; Boxer, S. G. *J. Phys. Chem. B* **1998**, *102*, 9148.
(28) Moore, L. J.; Zhou, H.; Boxer, S. G. *Biochemisty* **1999**, *38*, 11949.
(29) Lao, K.; Moore, L. J.; Zhou, H.; Boxer, S. G. *J. Phys. Chem.* **1995**, *99*, 496.
(30) Boxer, S. G.; Goldstein, A.; Lockhart, D. J.; Middendorf, T. R.; Takiff, L. *J. Phys. Chem.* **1989**, *93*, 8280.
(31) *Stark spectroscopy of photosynthetic systems*; Boxer, S. G., Ed.; Kluwer Academic: Dordrecht, The Netherlands, 1996; p 177.
(32) Cohen-Bazire, G.; Sistrom, W. R.; Stanier, R. Y. *J. Cell. Comput. Physiol* **1957**, *49*, 25.
(33) Marui, T.; Yamada, T.; Kobayashi, T.; Hashimoto, H. *Carotenoid Sci.* **2001**, *4*, 76.
(34) Gebhard, R.; van der Hoef, K.; Lefeber, A. W. M.; Erkelens, C.; Lugtenburg, J. *Recl. Trav. Chim. Pay-Bas* **1990**, *109*, 378.
(35) Gebhard, R.; van Dijk, J. T. M.; van Ouwerkerk, E.; Boza, M. V. T. J.; Lugtenburg, J. *Recl. Trav. Chim. Pay-Bas* **1991**, *110*, 459.
(36) Hashimoto, H.; Nakashima, T.; Hattori, K.; Yamada, T.; Mizoguchi, T.; Koyama, Y.; Kobayashi, T. *Pure. Appl. Chem* **1999**, *71*, 2225.
(37) Yanagi, K.; Kobayashi, T.; Hashimoto, H. *Phys. Rev. B* **2003**, *67*, 115122.
(38) Köler, M.; Friedrich, J.; Fidy, J. *Biochim. Biophys. Acta* **1998**, *1386*, 255.
(39) Scherer, P. O. J.; Fischer, S. F. *Chem. Phys. Lett* **1986**, *131*, 153.
(40) Krawczyk, S.; Olszówka, D. *Chem. Phys* **2001**, *265*, 335.
(41) Wortmann, R.; Elich, K.; Liptay, W. *Chem. Phys* **1988**, *124*, 395.
(42) Yanagi, K.; Hashimoto, H.; Gardinar, A. T.; Cogdell, R. J. *Phys. Rev. B* **2004**, *69*, *205103*.
(43) Palacios, M. A.; Frese, R. N.; Gradinaru, C. C.; van Stokkum, I. H. M.; Premvardhan, L. L.; Horton, P.; Ruban, A. V.; van Grondelle, R.; van Amerongen, H. *Biochim. Biophys. Acta* **2003**, *1605*, 83.
(44) Krawczyk, S.; Krupa, Z.; Maksymiec, W. *Biochim. Biophys. Acta* **1993**, *1143*, 273.
(45) Gottfried, D. S.; Steffen, M. A.; Boxer, S. G. *Science* **1991**, *251*, 662.
(46) Gottfried, D. S.; Stocker, J. W.; Boxer, S. G. *Biochim. Biophys. Acta* **1991**, *1059*, 63.
(47) Misawa, K.; Minoshima, K.; Ono, H.; Kobayashi, T. *Chem. Phys. Lett.* **1994**, *220*, 251.
(48) Misawa, K.; Kobayashi, T. *Nonliner Opt.* **1994**, *14*, 103.
(49) Woodbury, N. W.; Allen, J. P. The pathway, kinetics and thermodynamics of electron transfer in wild type and mutant reaction centers of purple nonsulfur bacteria. In *Anoxygenic photosynthetic bacteria*; Blankenship, R. E., Madigan, M. T., Bauer, C. E., Eds.; Kluwer Academic Publishers: The Netherlands, 1995; p 527.
(50) Cogdell, R. J.; Celis, S.; Crofts, A. R. *FEBS. Lett.* **1977**, *80*, 190.
(51) Farhoosh, R.; Chynwat, V.; Gebhard, R.; Lugtenburg, J.; Frank, H. A. *Photochem. Photobiol.* **1997**, *66*, 97.
(52) Feyman, R. P. Lectures on Physics. In *Lectures on Physics*; Addision-Wesley Publishing Company: London, 1965; Vol. 2.
(53) Humphrey, W.; Dalke, A.; Schulten, K. *J. Mol. Graph.* **1996**, *14*, 33.